

Article

Is ATP the Only Nucleoside Triphosphate among ATP, CTP, GTP, and UTP to Have a Role in Kinase Catalysis of Heme-Regulated Inhibitor toward eIF2 α during Lung Cancer Development?

Jakub Vávra , Artur Sergunin, Alžběta Farná, Tomáš Ovad , Toru Shimizu and Markéta Martínková * 

Department of Biochemistry, Faculty of Science, Charles University, Hlavova (Albertov) 2030-8, 128 43 Prague 2, Czech Republic

* Correspondence: marketa.martinkova@natur.cuni.cz

Abstract: The heme-regulated eukaryotic initiation factor 2 α (eIF2 α) kinase, also known as heme-regulated inhibitor (HRI), detects misfolded proteins and induces cytoprotective response to stress, mainly caused by heme-shortage. The nucleoside triphosphate ATP serves as the main donor of phosphate for the phosphorylation of eIF2 α by HRI in human cells. However, the other main nucleoside triphosphates (CTP, GTP, UTP) are also present at relatively high concentrations, especially in human tumor cells. Therefore, in this short communication we evaluate the role of four substrates (namely ATP, CTP, GTP, and UTP) on human HRI kinase activity. Additionally, for the first time, we perform a detailed kinetics study of the HRI G202S mutant, whose presence in the human lung is associated with cancer development. Here, the role of all four tested nucleoside triphosphates during cancer development is discussed from the point of view of the HRI activity. The results showed that the *k_{cat}* value of GTP was lower than that of ATP but was significantly higher than those of CTP and UTP. Additionally, the *k_{cat}* value of GTP for G202S was approximately 20% higher than that for wild-type, while the *k_{cat}* values of ATP, CTP, and UTP for G202S were lower than those for wild-type.

Keywords: Heme-based sensor; eukaryotic initiation factor 2 α ; eukaryotic initiation factor 2 α kinase; heme regulated inhibitor; intramolecular catalytic regulation; signal transduction



Citation: Vávra, J.; Sergunin, A.; Farná, A.; Ovad, T.; Shimizu, T.; Martínková, M. Is ATP the Only Nucleoside Triphosphate among ATP, CTP, GTP, and UTP to Have a Role in Kinase Catalysis of Heme-Regulated Inhibitor toward eIF2 α during Lung Cancer Development? *Catalysts* **2023**, *13*, 281. <https://doi.org/10.3390/catal13020281>

Academic Editor: Evangelos Topakas

Received: 11 December 2022

Revised: 22 January 2023

Accepted: 24 January 2023

Published: 27 January 2023



Copyright: © 2023 by the authors. Licensee MDPI, Basel, Switzerland. This article is an open access article distributed under the terms and conditions of the Creative Commons Attribution (CC BY) license (<https://creativecommons.org/licenses/by/4.0/>).

1. Introduction

Maintaining homeostasis during conditions of stress is a key requirement of all cells. The termination of translation represents one method employed to survive such stresses. Phosphorylation of the eukaryotic initiation factor 2 (eIF2) is the best-known translation control mechanism. During stress, any of the five specific protein kinases catalyze the phosphorylation of eIF2 on its α -subunit at Ser51, and the phosphate group is donated from ATP bound to the stress-activated kinase enzymes [1,2].

Among the eIF2 α kinases, Fe(III)-protoporphyrin IX complex (heme)-regulated inhibitor (HRI) [3], which is activated in response to a shortage of heme, was discovered first. This was followed by protein kinase R, where R denotes RNA-activated (PKR). PKR phosphorylates eIF2 α in response to double-stranded RNA produced during viral replication, thereby blocking the translation of viral mRNAs, as well as in response to signals such as oxidative and endoplasmic reticulum (ER) stress [4]. Thereafter, general control nonderepressible 2 kinase (GCN2) was discovered and found to be activated by binding of uncharged tRNAs, which accumulate as a result of the depletion of their cognate amino acids [5]. The protein kinase R-like endoplasmic reticulum kinase (PERK), which is mainly activated following the accumulation of misfolded proteins in the ER, was discovered next [6]. Finally, the fifth kinase phosphorylating eIF2 α , microtubule affinity-regulating kinase 2 (MARK2), was discovered more recently [7].

Heme shortage caused by inappropriate heme synthesis induces high levels of cell stress. HRI, which is abundantly expressed in erythroid cells, becomes activated under such conditions, preventing the accumulation of inactive (misfolded) globin with no heme co-factor [8,9]. HRI is composed of two domains, namely, the N-terminal sensing domain and the C-terminal kinase domain, containing a unique kinase insert region [10,11]. One molecule of heme is bound to the full-length protein [12]. His119/His120, located in the sensing domain, and Cys409 (part of the heme-regulatory Cys/Pro motif), located in the kinase domain, are the axial ligands for the heme in HRI [10,11,13]. HRI has a moderate affinity for heme, which allows it to sense the heme concentration in the cell. Other compounds have also been found to inhibit HRI kinase activity [12,14]. Moreover, recent studies have demonstrated the roles of HRI in cells other than reticulocytes [15], indicating that HRI not only detects heme deprivation, but also the misfolding of cytosolic proteins and mitochondrial defects to induce chaperones, analogous to the role of PERK in response to ER stress/misfolding [16,17]. Aside from the response to heme shortage, the other regulatory roles of HRI are probably associated with chaperone interactions [18] and/or regulation of HRI autophosphorylation [19]. A previous kinetics study showed that the HRI kinase reaction follows classical Michaelis-Menten kinetics with respect to ATP, and sigmoidal kinetics and positive cooperativity between subunits with respect to the protein substrate (eIF2 α) [12].

ATP is the main donor of phosphate to phosphorylate eIF2 α at Ser51 [12]. However, as other nucleoside triphosphates (CTP, GTP, UTP) are also present at high concentrations in human cells, they may also be utilized by HRI [20]. Moreover, a specific mutation of HRI, namely G202S, has been reported to be associated with lung cancer development [21]. This mutation is proposed to influence HRI affinity to ATP, given that the mutation position is located close to the supposed ATP binding site, which is targeted by many HRI activators and/or inhibitors [22].

Therefore, in this study, we sought to investigate the ways in which the main cellular nucleoside triphosphates (ATP, CTP, GTP, and UTP) influence the kinase reaction of wild-type (WT) human HRI and its G202S mutant.

2. Results

The various nucleoside triphosphates commonly present in human cells were compared for their ability to serve as a substrate for the eIF2 α kinase reaction catalyzed by either the human HRI WT enzyme or its G202S mutant form. The time courses of the eIF2 α phosphorylation catalyzed by the HRI WT enzyme and its G202S mutant form in the presence of various nucleoside triphosphates were similar (Figure 1A,B). However, we observed marked differences in the kinase activities between reactions with purine nucleoside triphosphates (ATP, GTP; Figure 1, black and red points and lines) and pyrimidine nucleoside triphosphates (CTP, UTP; Figure 1, green and blue points and lines), suggesting that the purine nucleoside triphosphates play a critical role in the activity of HRI.

We next conducted a detailed kinetics analysis of the eIF2 α phosphorylation by the HRI WT and the HRI G202S mutant to determine the role, if any, of the various nucleoside triphosphates in the catalytic process. As the kinase reaction catalyzed by HRI involves two substrates (a nucleoside triphosphate and eIF2 α), we measured the apparent kinetics parameters for each of the tested nucleoside triphosphate substrates in the presence of an excess of eIF2 α (Figure 2A–D and Table 1). The phosphorylation of eIF2 α catalyzed by both the HRI WT enzyme and the HRI G202S mutant showed classical Michaelis-Menten kinetics with respect to the ATP, GTP, and UTP concentration (Figure 2A–D). In contrast, the enzyme reaction catalyzed by the HRI G202S mutant in the presence of CTP showed sigmoidal kinetics with respect to the CTP concentration (Figure 2B, red points and line), while the similar reaction catalyzed by the HRI WT enzyme followed classical Michaelis-Menten kinetics (Figure 2B, black points and line).

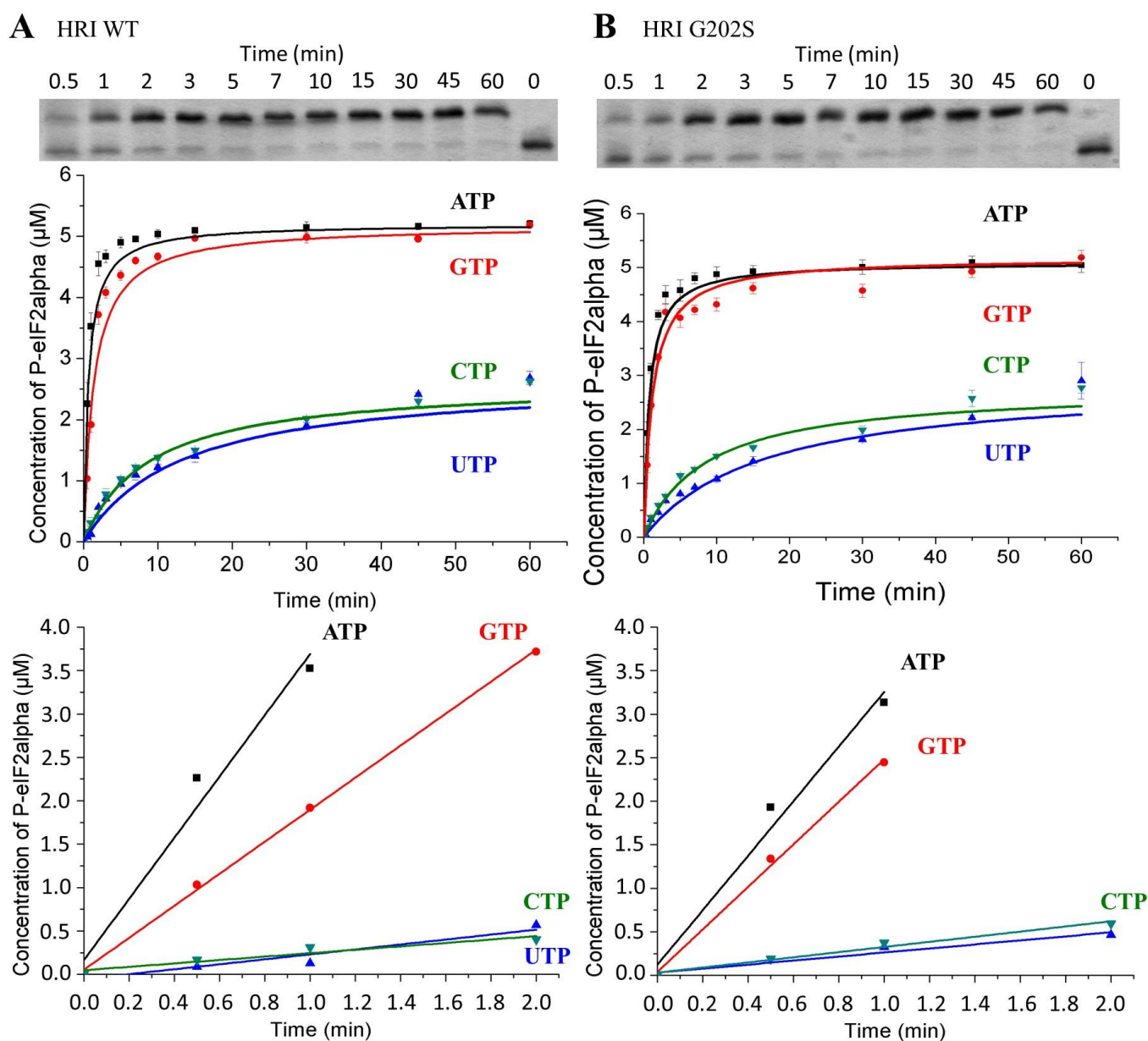


Figure 1. Time course of eIF2 α phosphorylation catalyzed by the HRI WT enzyme (**A**) and the HRI G202S mutant (**B**) in the presence ATP (black), CTP (green), GTP (red), and UTP (blue) at $900 \mu\text{mol}\cdot\text{L}^{-1}$ concentration. The bars in the graphs indicate standard deviations for each experimental point from at least three independent experiments. The insets above both graphs show an example of raw data representing a single experiment and determination of the phosphorylated form of eIF2 α (higher bands) as estimated at various time points formed by HRI with ATP as a substrate. The insets below both graphs are prepared by zooming the presented functions into the initial times to demonstrate the linear section of the curves—1 min for ATP and GTP and 2 min for CTP and UTP.

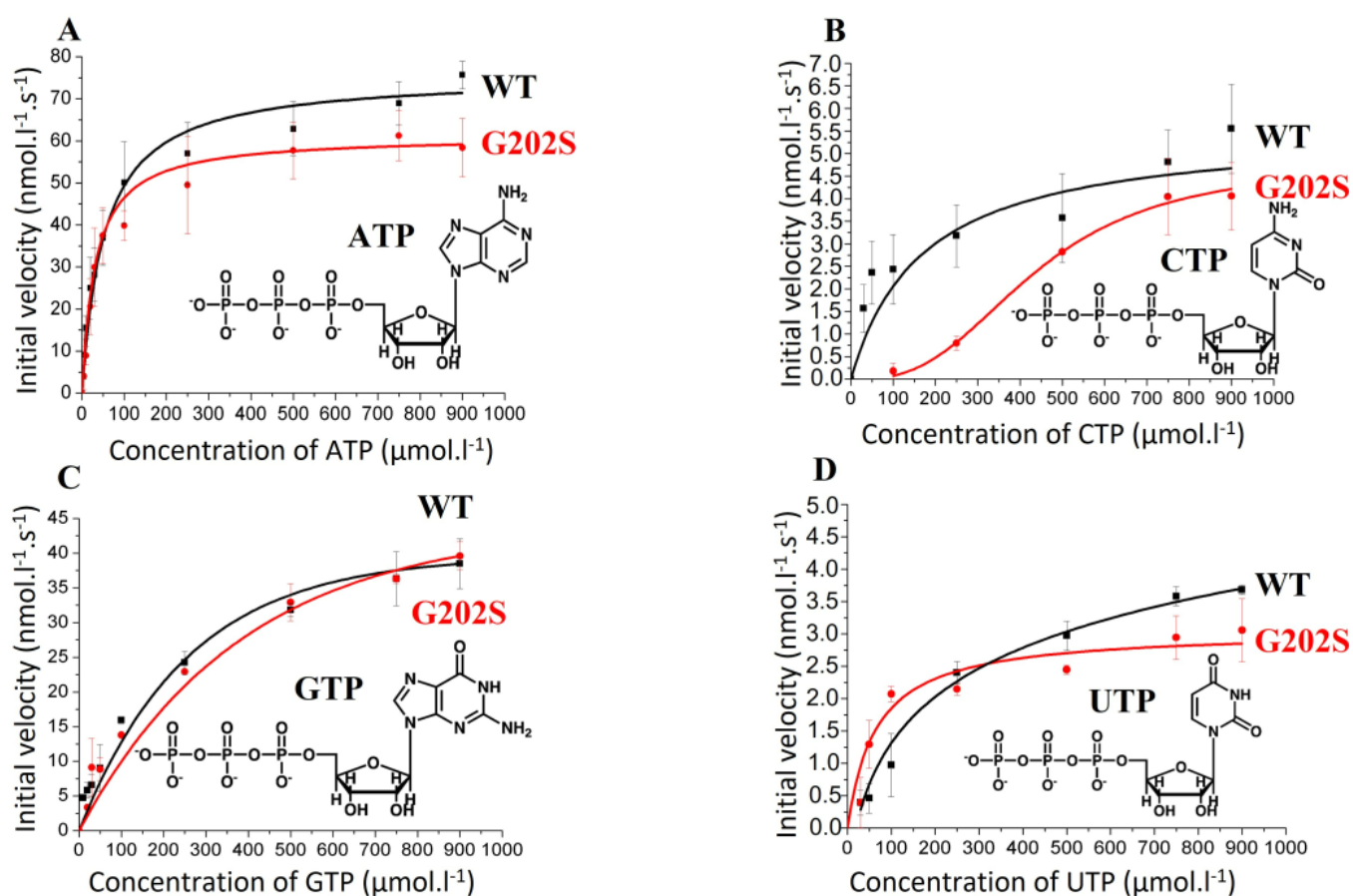


Figure 2. Initial velocity of the eIF2 α phosphorylation catalyzed by the HRI WT enzyme (black) and the HRI G202S mutant (red) as a function of ATP (A), CTP (B), GTP (C), and UTP (D) concentration. The bars in the graphs indicate standard deviations for each experimental point from at least three independent experiments.

Table 1. Apparent kinetic parameters, catalytic constants (turnover numbers) and catalytic efficiency values of the HRI reaction for the various nucleoside triphosphates.

	HRI WT	HRI G202S
K_M^{ATP} (μM)	25 ± 5	49 ± 13
$V_{\text{max}}^{\text{ATP}}$ ($\text{nM}\cdot\text{s}^{-1}$)	75 ± 6	62 ± 5
$k_{\text{cat}}^{\text{ATP}}$ (min^{-1})	12.8	10.6
$k_{\text{cat}}^{\text{ATP}}/K_M^{\text{ATP}}$ ($\text{mM}^{-1}\cdot\text{min}^{-1}$)	514	217
$K_{0.5}^{\text{CTP}}$ (μM)	368 ± 74	380 ± 76
$V_{\text{max}}^{\text{CTP}}$ ($\text{nM}\cdot\text{s}^{-1}$)	7.1 ± 0.6	4.0 ± 0.3
$k_{\text{cat}}^{\text{CTP}}$ (min^{-1})	1.22	0.69
$k_{\text{cat}}^{\text{ATP}}/K_{0.5}^{\text{CTP}}$ ($\text{mM}^{-1}\cdot\text{min}^{-1}$)	3.31	1.81
K_M^{GTP} (μM)	135 ± 43	240 ± 77
$V_{\text{max}}^{\text{GTP}}$ ($\text{nM}\cdot\text{s}^{-1}$)	40 ± 14	47 ± 18
$k_{\text{cat}}^{\text{GTP}}$ (min^{-1})	6.86	8.06

Table 1. Cont.

	HRI WT	HRI G202S
$k_{\text{cat}}^{\text{ATP}}/K_{\text{M}}^{\text{GTP}}$ ($\text{mM}^{-1}\cdot\text{min}^{-1}$)	50.8	33.6
$K_{\text{M}}^{\text{UTP}}$ (μM)	37 ± 5	29 ± 6
$V_{\text{max}}^{\text{UTP}}$ ($\text{nM}\cdot\text{s}^{-1}$)	3.5 ± 0.5	2.9 ± 0.2
$k_{\text{cat}}^{\text{UTP}}$ (min^{-1})	0.60	0.50
$k_{\text{cat}}^{\text{ATP}}/K_{\text{M}}^{\text{UTP}}$ ($\text{mM}^{-1}\cdot\text{min}^{-1}$)	16.2	17.1

K_{M} : Michaelis constant resp. apparent Michaelis constant with regard to the indicated substrate, V_{max} : Maximal velocity resp. apparent Maximal velocity with regard to the indicated substrate, $K_{0.5}^{\text{CTP}}$: values were obtained from the sigmoidal dose-response curve for CTP, where the Michaelis/Menten kinetics cannot be applied; k_{cat} : Catalytic constant resp. turnover number with regard to the indicated substrate.

Compared to the HRI WT enzyme, the HRI G202S mutant variant showed either comparable maximal enzymatic velocity values ($V_{\text{max}}^{\text{ATP}}$, $V_{\text{max}}^{\text{CTP}}$, $V_{\text{max}}^{\text{GTP}}$, and $V_{\text{max}}^{\text{UTP}}$ values) or slight decreases in all conditions tested (Figure 2 and Table 1). Consistently, the apparent Michaelis constants and the corresponding apparent $K_{0.5}$ constant increased for the HRI G202S mutant compared to the HRI WT enzyme for ATP, CTP, and GTP ($K_{\text{M}}^{\text{ATP}}$, $K_{0.5}^{\text{CTP}}$, $K_{\text{M}}^{\text{GTP}}$) values, suggesting lower affinity of the HRI G202S mutant than the HRI WT enzyme to the corresponding nucleoside triphosphates (Figure 2A–C and Table 1). Surprisingly, the opposite situation was observed for the HRI kinase reaction in the presence of UTP (Figure 2D and Table 1). The apparent Michaelis constant decreased for the HRI G202S mutant compared to the HRI WT enzyme with regard to UTP ($K_{\text{M}}^{\text{UTP}}$), suggesting slightly higher affinity of the HRI G202S mutant to UTP than was observed for the HRI WT.

The results also showed that the V_{max} value with GTP ($40 \text{ nM}\cdot\text{s}^{-1}$) was lower than that of ATP ($75 \text{ nM}\cdot\text{s}^{-1}$) for the WT HRI, but was significantly higher than those of the other nucleoside triphosphates, CTP ($7.1 \text{ nM}\cdot\text{s}^{-1}$) and UTP ($3.5 \text{ nM}\cdot\text{s}^{-1}$). Additionally, the V_{max} value ($47 \text{ nM}\cdot\text{s}^{-1}$) with GTP for the G202S mutant was higher than that ($40 \text{ nM}\cdot\text{s}^{-1}$) for the WT, reinforcing that GTP is a likely substitute ATP for G202S (Table 1). The WT enzyme was found to be more effective than the mutant form, regardless of the type of nucleoside triphosphate. Interestingly, despite the effectiveness of the mutant being approximately half that of the WT HRI in the case of ATP, CTP, and GTP, in the case of UTP, the WT and mutant enzymes were similarly effective. This is likely because the affinity of the G202S mutant to UTP is slightly higher than that of the HRI WT enzyme (Table 1).

HRI, as a typical heme-responsive sensor enzyme, can detect changes in heme concentration. A sufficiently high heme concentration can inhibit the eIF2 α kinase reaction. We examined the heme-mediated inhibition of the HRI WT enzyme and the HRI G202S mutant kinase reactions utilizing nucleoside triphosphates. As summarized in Table 2, we found no significant difference in the sensitivity to heme inhibition (IC_{50} values) for the two forms of HRI tested. However, when ATP served as a substrate of the kinase reaction, the HRI G202S mutant was slightly more sensitive to heme inhibition compared to the HRI WT enzyme (Figure 3).

Table 2. Extent of heme-induced HRI inhibition utilizing various nucleoside triphosphates, expressed as IC_{50} values.

	$\text{IC}_{50}^{\text{ATP}}$ (μM)	$\text{IC}_{50}^{\text{CTP}}$ (μM)	$\text{IC}_{50}^{\text{GTP}}$ (μM)	$\text{IC}_{50}^{\text{UTP}}$ (μM)
HRI WT	14 ± 5	10	10 ± 4	10
HRI G202S	11 ± 4	10	11 ± 4	10

IC_{50} : Half maximal inhibitory concentration.

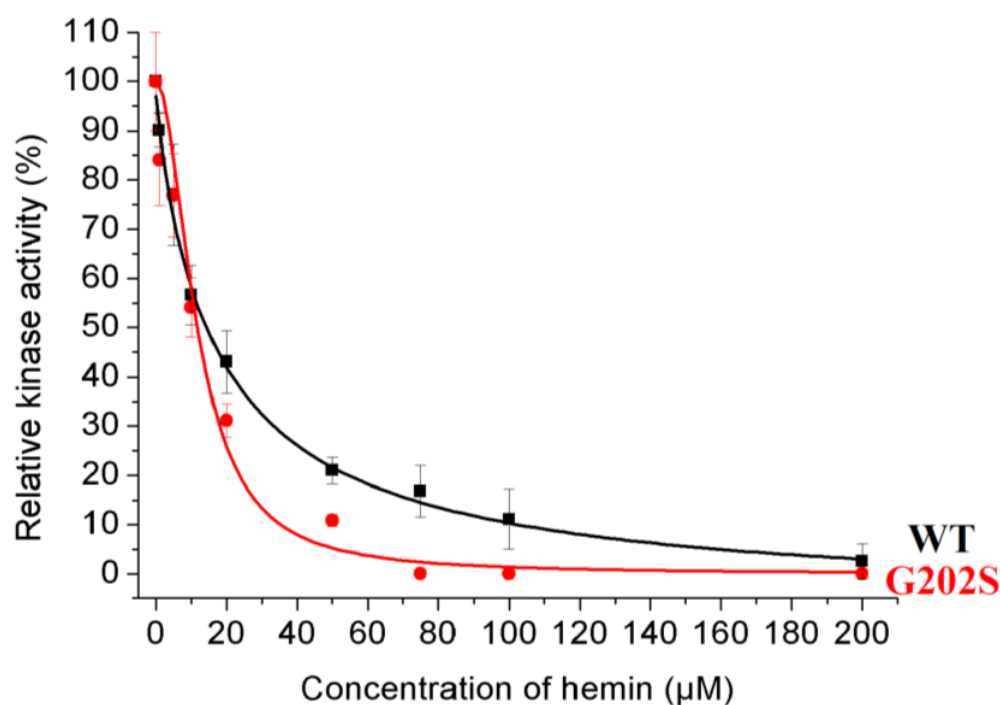


Figure 3. Inhibition of HRI WT (black) and HRI G202S (red) enzymes by various concentrations of heme in the presence of $900 \mu\text{mol}\cdot\text{l}^{-1}$ ATP. Heme was dissolved in dimethyl sulfoxide (DMSO) to yield final concentrations of 0.5–200 μM . An equal volume of DMSO alone was added to the control reaction mixture.

3. Discussion

Purine nucleoside triphosphates play a critical role in the activity of HRI, either the WT enzyme or the G202S mutant, and, unexpectedly, pyrimidine nucleoside triphosphates can also serve as a source of phosphate for the eIF2 α kinase reaction. The *in vitro* properties of some kinase enzymes (i.e., casein kinase I and II) suggest that ATP is not the only, or not even the major, phosphate donor, and may also be reflected *in vivo* [20]. In case of the HRI kinase reaction, ATP, closely followed by GTP, are the major phosphate donors for the phosphorylation of eIF2 α . However, during stress, when the amount of ATP or GTP is limited by their utilization in other processes, the effects of CTP and UTP on the HRI kinase reaction cannot be underestimated. Nucleoside triphosphate levels in normal (resting) cells are lower than those in tissues. However, the levels of nucleoside triphosphates, particularly those of CTP, GTP, and UTP relative to ATP, are significantly higher in tumor cells [20]. In human myeloid leukemia cells, the concentration of ATP is estimated as ~ 3.5 mM, while that of CTP, GTP, and UTP are estimated as ~ 0.4 mM, ~ 0.9 mM, and ~ 0.9 mM, respectively [23]. However, it has been reported that the concentrations of a given nucleoside triphosphate in the same cell line or tissue vary over a range of 5–50-fold under various circumstances [24]. Even for the basal nucleoside triphosphate concentrations, all of the obtained apparent K_M^{NTP} or $K_{0.5}^{\text{NTP}}$ are relevant and the kinase enzyme reaction may proceed following the participation of all four nucleoside triphosphates. It should be noted that native human HRI works at 37 °C and our kinetics experiments were performed at 20 °C, because of the enzyme stability. Anyway, we believe that even if the specific values for ATP, CTP, GTP, and UTP and their affinities to HRI may differ at various temperatures, their mutual relationship and indicated behavior are similar at 20 and 37 °C. Moreover, heme still inhibits enzyme activity even if the pyrimidine nucleoside triphosphates are used, and the heme sensing role of HRI is not disrupted by the other utilized source of phosphate. However, because the concentrations of heme and nucleotides utilized in the experimental setting were three orders of magnitude higher compared to the HRI concentration, an interaction between nucleotides and heme cannot be excluded and if so, such an interaction

is not competitive to HRI–heme and HRI–nucleotide interactions. Such a situation could hypothetically impact the precision of data. If heme interacts with nucleotides, it lowers its available concentration. Presented data only provide a rough idea what the ratios of IC_{50} values are potentially like.

As mentioned above, HRI has been suggested to play a role in cancer development [15]. The phosphorylation of eIF2 α catalyzed by HRI causes proteosynthesis to be turned off, and therefore represents a cytoprotective response to stress conditions, which can be disturbed by the malignant transformation of cell. Systematic sequencing of cancer genomes for mutations showed that human cancer cells (mainly lung cells) often possess a mutation in the HRI gene, which causes expression of the G202S mutant variant of the HRI enzyme [21]. As this mutation site is located close to the ATP binding site, we sought to analyze this pathologically relevant mutation for the first time by conducting a detailed enzyme kinetics study. Our results suggest that glycine 202 is slightly involved in the ATP binding process, given that its replacement by a serine increased the K_M^{ATP} by two-fold, suggesting a decrease in ATP affinity of the HRI G202S mutant form. Consistently, the maximal enzyme velocity was slightly decreased for the HRI G202S mutant form, while a similar situation was observed for the other purine nucleoside triphosphate, GTP.

However, the situation with the pyrimidine nucleoside triphosphates is different. The affinity of HRI for CTP is not significantly influenced by the mutation of G202, the $K_{0.5}^{CTP}$ (obtained from the sigmoidal function) was also very high, even for the HRI WT enzyme, and a similarly high value was observed for the mutant protein. Despite the high $K_{0.5}^{CTP}$, the reaction still proceeded slowly but effectively, and the eIF2 α was still phosphorylated. Interestingly, we have observed the sigmoidal curve shape only for CTP only in the case of the HRI G202S. We think that the amino groups on the purine position 6 and pyrimidine position 4 in ATP and CTP, respectively could be the key to explain that sigmoidal observation. Because the important glycine 202 is mutated to serine in HRI G202S, the interaction with that pyrimidine nucleotide is changed causing the different behavior of the kinetics function. However, the possibility that the level of enzyme reaction is in this case so low, that the measurement is laden with great experimental error could also not be ruled out. However, in the case of UTP, the G202S mutation associated with cancer development slightly increased the affinity of the HRI to UTP compared to the HRI WT enzyme. It is currently unclear how this phenomenon could be directly connected to the carcinogenesis. It may be that UTP can then compete with ATP for the binding site and cause the disbalance of the eIF2 α phosphorylation process. Further studies will be necessary to fully understand the role of all four major nucleoside triphosphates in cancer cells. It is also important to note that although the HRI G202S mutant is sensitive to heme inhibition, it is slightly more sensitive compared to the HRI WT enzyme when ATP serves as a substrate for the kinase reaction.

According to a previous study, the current research was performed with a human HRI protein [25], although previous research focused mainly on the murine variant of the protein [12]. It seems that both variants behave in a similar manner (human HRI K_M^{ATP} $25 \pm 5 \mu\text{M}$, mouse HRI K_M^{ATP} $31 \mu\text{M}$). Additionally, the sensitivity to heme inhibition is comparable (human HRI IC_{50} $14 \pm 5 \mu\text{M}$, murine HRI IC_{50} $9.5 \mu\text{M}$), although the human HRI is slightly less sensitive to heme compared to the murine HRI. Interestingly, the recent study with human HRI protein showed approximately three-fold lower affinity to ATP (human HRI K_M^{ATP} $71.9 \mu\text{M}$) but higher sensitivity to hemin (IC_{50} $0.9 \mu\text{M}$), which is probably caused by different human HRI constructs, protein manipulation, different methods of HRI activity assay, and the utilization of a short peptide derived from eIF2 α instead of the WT substrate used in the current study [25].

It should also be noted that we have only studied the kinase reaction of HRI towards eIF2 α , despite the fact that HRI is known to also catalyze its autophosphorylation [12,19]. The autophosphorylation of HRI is a multistep process [19], which is important for adequate solubility of the protein in aqueous media [12]. As we successfully expressed and isolated

the HRI protein, the protein used in the present study is likely to be soluble due to its previous autophosphorylation, which took place during its expression in *E. coli* cells.

Four other eIF2 α kinases (PRK, GCN2, PERK, and MARK2) are able to phosphorylate this initiation factor and arrest translation [2,4–7]. So far, only PERK has been analyzed in terms of the apparent K_M^{ATP} and V_{max}^{ATP} of the eIF2 α kinase reaction. The apparent Michaelis constant with regards to ATP was $1.08 \pm 0.21 \mu\text{M}$, and the apparent maximal velocity with regards to ATP was $0.88 \pm 0.22 \text{ pmol}\cdot\text{min}^{-1}$ [26]. The PERK functional kinase domain has approximately one order of magnitude higher affinity to ATP compared to HRI, while the maximal enzyme velocities are comparable. In the case of PKR, only its autophosphorylation reaction was studied [27], and there remains no information regarding GCN2 and MARK2 kinetics.

Finally, targeting eIF2 α kinases, including HRI, with pharmacological inhibitors and/or activators to shift the balance toward a cytotoxic state and/or an apoptotic state, specifically in cancer cells, may provide an alternative approach in anticancer therapy [1,15]. The current study shed light on the mechanism of the eIF2 α kinase reaction catalyzed by HRI enzyme while also outlining novel directions for future research on eIF2 α phosphorylation.

4. Materials and Methods

4.1. Materials

Ampicillin was obtained from P-lab (Prague, Czech Republic). Isopropyl β -D-thiogalactopyranoside, hemin, and acrylamide were obtained from Sigma-Aldrich (St. Louis, MO, USA). Water, doubly distilled over quartz, was purified using a Milli-Q Plus system (EMD Millipore, Billerica, MA, USA). Phos-tag was obtained from the Phos-tag consortium Wako Pure Chemical Industries (Osaka, Japan). All chemicals used were of the highest purity grade available from commercial sources and did not undergo further purification.

4.2. Plasmid Construction

The gene for human HRI was obtained from the repository PlasmID of the Harvard Medical School (Boston, MA, USA). The following primers were used for the gene amplification and its insertion into the pET-21c(+) vector: 5'-sense (5'-AGATACATATGCAGGGGGGCAACTC-3') and 3'-antisense (5'-AGATACTCGAGCTATCCCACGCCCCCATC-3'). Following gene amplification, the plasmid encoding human (His)₆-tagged WT HRI, comprising residues 1–630, was obtained. A site-directed mutant HRI G202S was constructed with the QuikChange II Site-Directed Mutagenesis Kit (Agilent Technologies, Santa Clara, CA, USA) using the following primers: 5'-sense (5'-GCAATAAAAAAAAAATCCTGATTAAGAGTGCAACTAAAACAGTTTG-3') and 3'-antisense (5'-CAAAGTGTGTTTGTGCACTCTTAATCAGGATTTTTTTTATTGC-3').

The gene for human eIF2 α was obtained from the repository of the Harvard Medical School (PlasmID, USA). The following primers were used for the gene amplification and its insertion into the pET-21c(+) vector: 5'-sense (5'-AGATACATATGCCGGGTCTAAGTTGTAG-3') and 3'-antisense (5'-AGATACTCGAGCAAATCTTCAGCTTTGGCTTC-3'). Following gene amplification, the plasmid encoding human (His)₆-tagged WT eIF2 α , comprising residues 1–315, was obtained.

4.3. Overexpression and Purification of the WT and Mutant Proteins

The (His)₆-tagged HRI WT enzyme and its mutant G202S were expressed upon addition of 0.1 mM isopropyl β -D-thiogalactopyranoside in *Escherichia coli* BL21(DE3) (Novagen) harboring pET-21c(+)-HRI WT and pET-21c(+)-G202S HRI, respectively and then purified as described previously [12] with some modifications. Briefly, the cells were resuspended in buffer A (50 mM Tris-HCl pH 8.0, 100 mM NaCl) containing 1 mM phenylmethanesulfonyl fluoride and 1 mM ethylenediaminetetraacetic acid and lysed with 0.2 mg·ml⁻¹ lysozyme. The crude extract was sonicated six times for 1 min each (with 1 min intervals between sonications) on ice and then centrifuged at 50,000 g for 60 min at 4 °C. The resulting supernatant

was then incubated with 3 mL of TALON[®] SuperFlow (GE Healthcare, Sweden) affinity resin (buffer A pre-equilibrated) for 60 min at 4 °C. Following incubation, the mixture was applied onto a column glass reservoir with fritted glass at its end. After washing the mixture with buffer A, the HRI protein was eluted with 200 mM imidazole in buffer A. The fraction of eluted HRI was concentrated with Amicon[®] Ultra Centrifugal Filters (Merck Millipore, Cork, Ireland) and applied to a Superdex 200 10/300 GL column (GE Healthcare, Amersham, UK) equilibrated with 20 mM Tris-HCl pH 8.0 buffer containing 150 mM NaCl. The desired eluates (identified by monitoring at 280 nm) were collected and concentrated with Amicon[®] Ultra Centrifugal Filters (Merck Millipore, Cork, Ireland). Finally, the purified proteins were rapidly frozen in liquid nitrogen and stored at −80 °C. The purified proteins were more than 95% homogeneous as determined by sodium dodecyl sulfate-polyacrylamide gel electrophoresis (SDS-PAGE; 10% gel) followed by staining with InstantBlue[®] Coomassie Protein Stain (Abcam, Cambridge, UK). The protein concentrations were determined using the bicinchoninic acid assay with bovine serum albumin as a standard (Pierce[™] BCA Protein Assay Kit, Thermo Scientific, Rockford, IL, USA). The final yields for the full-length HRI WT enzyme and the HRI G202S mutant were 0.5 and 0.2 mg/L of culture, respectively.

(His)₆-tagged eIF2 α was expressed upon addition of 0.1 mM isopropyl β -D-thiogalactopyranoside in *Escherichia coli* BL21(DE3) (Novagen) harboring pET-21c(+)-eIF2 α plasmid. The purification process was identical to that described for HRI. The purified eIF2 α protein was more than 97% homogeneous as determined by SDS-PAGE followed by staining with InstantBlue[®] Coomassie Protein Stain (Abcam, Cambridge, UK). The protein concentrations were determined using the bicinchoninic acid assay with bovine serum albumin as a standard (Pierce[™] BCA Protein Assay Kit, Thermo Scientific, Rockford, IL, USA). The final yield of eIF2 α protein was 1.2 mg/L of culture.

4.4. HRI Reaction Kinetics under Various Conditions

The time course of the kinase reaction catalyzed by the HRI WT enzyme and the HRI G202S mutant was assayed at 20 °C in a reaction mixture containing 0.35 μ M HRI WT enzyme or its G202S mutant and 5.4 μ M eIF2 α proteins in 20 mM Tris-HCl, pH 8, containing 2 mM MgCl₂ and 60 mM KCl. The reaction mixture was preincubated for 5 min before initiating the reaction by adding 900 μ M ATP, CTP, GTP, or UTP at 20 °C. The state of the reaction was determined at the following time points after initiation: 0, 0.5, 1, 2, 3, 5, 7, 10, 15, 30, 45, and 60 min.

The kinetics analysis of the HRI WT enzyme and the HRI G202S mutant was conducted under various conditions. Unless stated otherwise, the experiments were performed at 20 °C. The reaction mixture (20 μ L) for the kinetics analysis of HRI contained 20 mM Tris-HCl, pH 8, 2 mM MgCl₂, 60 mM KCl, 0.35 μ M HRI WT enzyme or its G202S mutant, and 5.4 μ M eIF2 α proteins. The reaction mixture was preincubated for 5 min before initiating the reaction by adding 5–900 μ M ATP, CTP, GTP, or UTP.

The assay solution was incubated for 1 min (initial velocity conditions for ATP and GTP) or 2 min (initial velocity conditions for CTP and UTP). The amount of reaction product (phosphorylated eIF2 α , P-eIF2 α) formed per min during the first 1 min (ATP and GTP) or 2 min (CTP and UTP) was equivalent to the initial velocity of the kinase reaction. As the HRI kinase reaction is a bisubstrate reaction (between a nucleoside triphosphate and eIF2 α), the apparent kinetics for each nucleoside triphosphate were determined in the presence of an excess of the other substrate (eIF2 α). The kinetic constants were determined using a Lineweaver–Burk plot and in parallel by nonlinear least-squares regression analysis using the Michaelis–Menten equation or the Hill equation, as appropriate [28]. The experiments were performed at least three times for each assay solution, and the experimental errors were within 15%.

4.5. Identification of the P-eIF2 α by Phos-Tag Electrophoresis

At the designated times, the HRI kinase assay reaction was terminated by adding 20 μ L aliquots of termination buffer (250 mM Tris-HCl, pH 6.8, 8% SDS, 22% 2-mercaptoethanol, 50% glycerol, 0.004% bromophenol blue). Subsequently, the quenched reaction mixture samples were loaded onto a 10% SDS poly-acrylamide gel containing 75 μ M Phos-tag acrylamide and 0.2 mM MnCl₂. Each lane was loaded with a quantity of quenched reaction mixture containing 0.5 μ g of eIF2 α . The phosphorylated proteins in the sample interacted with the Phos-tag manganese complex in the gel, reducing their mobility relative to phosphate-free proteins [10,29]. Following electrophoresis, the proteins were visualized by staining with InstantBlue[®] Coomassie Protein Stain (Abcam, Cambridge, UK) and the stained gels were imaged using an Epson Perfection V550 scanner (Seiko Epson, Suwa, Japan). The loaded proteins were then quantified by analyzing the scanned images using ImageJ.

4.6. Heme Inhibition Studies

The heme inhibition studies of the HRI WT enzyme and its G202S were assayed under various conditions. Unless stated otherwise, the experiments were conducted at 20 °C. The reaction mixture (20 μ L) for the heme inhibition studies of HRI contained 20 mM Tris-HCl, pH 8, 2 mM MgCl₂, 60 mM KCl, 0.35 μ M HRI WT enzyme or its G202S mutant protein, 5.4 μ M eIF2 α protein, and 1–200 μ M heme dissolved in DMSO. The volume equivalent of DMSO alone was used as a control for no heme condition. The reaction mixture was preincubated for 5 min before initiating the reaction by adding 900 μ M ATP, CTP, GTP, or UTP.

The assay solution was incubated for 1 min (initial velocity conditions for ATP and GTP) or 2 min (initial velocity conditions for CTP and UTP). The amount of reaction product (P-eIF2 α) formed per min during the first 1 min (ATP and GTP) or 2 min (CTP and UTP) was equivalent to the initial velocity of the kinase reaction for each specific heme concentration in the assay solution. The relative kinase activity of HRI for each specific heme concentration in the assay solution was obtained by comparing the initial velocity of its kinase reaction with the kinase reaction of HRI in the absence of heme in the assay mixture. The IC₅₀ values were estimated from the relationship between the relative kinase activity of HRI and the heme concentration in the assay mixture. The experiments were performed at least three times for each reaction mixture, and the experimental errors were within 15%.

5. Conclusions

In summary, our results suggest that in case of the HRI kinase reaction, ATP, closely followed by GTP, are the major phosphate donors for the phosphorylation of eIF2 α . However, under certain stress conditions, the roles of CTP and UTP in the HRI kinase reaction cannot be underestimated. The WT enzyme is consistently more effective compared to the G202S mutant regardless the nucleoside triphosphate. In the case of ATP, CTP, and GTP, the mutant associated with lung cancer development is approximately half as effective as the WT HRI, while in the case of UTP, the WT and mutant enzymes show similar efficacy. The HRI G202S mutant shows decreased affinity to ATP, CTP, and GTP. However, in the case of UTP, the G202S mutant significantly increases the affinity to UTP compared to WT enzyme.

Author Contributions: Conceptualization, M.M. and T.S.; methodology, A.F. and J.V.; validation, A.S., T.O. and J.V.; formal analysis, A.F.; investigation, A.S., T.O. and J.V.; writing—original draft preparation, M.M. and J.V.; writing—review and editing, M.M. and T.S.; visualization, J.V. All authors have read and agreed to the published version of the manuscript.

Funding: This work was supported by The Ministry of Education, Youth and Sports [the grant number 8F20011] and the Grant Agency of the Charles University [the GAUK project number 158120].

Data Availability Statement: The study did not report any data.

Conflicts of Interest: The authors declare no conflict of interest.

Abbreviations

eIF2 α : Eukaryotic initiation factor 2 α , P-eIF2 α : Phosphorylated eIF2 α , HRI: Heme-regulated inhibitor or alternatively heme-regulated eukaryotic initiation factor 2 α kinase, PERK: Protein kinase R-like endoplasmic reticulum kinase, PKR: Protein kinase R (R denotes RNA-activated), GCN2: General control nonderepressible 2, MARK2: Microtubule affinity-regulating kinase 2, ATP: Adenosine triphosphate, CTP: Cytidine triphosphate, GTP: Guanosine triphosphate, UTP: Uridine triphosphate, tRNA: Transfer RNA, eIF: Eukaryotic initiation factor, ER: Endoplasmic reticulum, *k*_{cat}: Catalytic constant resp. turnover number, *K*_M: Michaelis constant, *V*_{max}: Maximal velocity, IC₅₀: Half maximal inhibitory concentration, SDS-PAGE: Sodium dodecyl sulfate–polyacrylamide gel electrophoresis, WT: Wild type, DMSO: dimethyl sulfoxide.

References

1. Wang, X.; Proud, C.G. The Role of EIF2 Phosphorylation in Cell and Organismal Physiology: New Roles for Well-Known Actors. *Biochem. J.* **2022**, *479*, 1059–1082. [[CrossRef](#)]
2. Colthurst, D.R.; Campbell, D.G.; Proud, C.G. Structure and Regulation of Eukaryotic Initiation Factor EIF-2. Sequence of the Site in the Alpha Subunit Phosphorylated by the Haem-Controlled Repressor and by the Double-Stranded RNA-Activated Inhibitor. *Eur. J. Biochem.* **1987**, *166*, 357–363. [[CrossRef](#)] [[PubMed](#)]
3. Ochoa, S. Regulation of Protein Synthesis. *Eur. J. Cell Biol.* **1979**, *19*, 95–101. [[CrossRef](#)]
4. Clemens, M.J. PKR—a Protein Kinase Regulated by Double-Stranded RNA. *Int. J. Biochem. Cell Biol.* **1997**, *29*, 945–949. [[CrossRef](#)]
5. Misra, J.; Holmes, M.J.; Mirek, T.E.; Langevin, M.; Kim, H.-G.; Carlson, K.R.; Watford, M.; Dong, X.C.; Anthony, T.G.; Wek, R.C. Discordant Regulation of EIF2 Kinase GCN2 and MTORC1 during Nutrient Stress. *Nucleic Acids Res.* **2021**, *49*, 5726–5742. [[CrossRef](#)] [[PubMed](#)]
6. Ron, D.; Harding, H.P. Protein-Folding Homeostasis in the Endoplasmic Reticulum and Nutritional Regulation. *Cold Spring Harb. Perspect. Biol.* **2012**, *4*, a013177. [[CrossRef](#)]
7. Lu, Y.-N.; Kavianpour, S.; Zhang, T.; Zhang, X.; Nguyen, D.; Thombre, R.; He, L.; Wang, J. MARK2 Phosphorylates EIF2 α in Response to Proteotoxic Stress. *PLoS Biol.* **2021**, *19*, e3001096. [[CrossRef](#)]
8. Chen, J.J.; London, I.M. Regulation of Protein Synthesis by Heme-Regulated EIF-2 Alpha Kinase. *Trends Biochem. Sci.* **1995**, *20*, 105–108. [[CrossRef](#)] [[PubMed](#)]
9. Shimizu, T.; Lengalova, A.; Martinek, V.; Martinková, M. Heme: Emergent Roles of Heme in Signal Transduction, Functional Regulation and as Catalytic Centres. *Chem. Soc. Rev.* **2019**, *48*, 5624–5657. [[CrossRef](#)]
10. Igarashi, J.; Murase, M.; Iizuka, A.; Pichierri, F.; Martinkova, M.; Shimizu, T. Elucidation of the Heme Binding Site of Heme-Regulated Eukaryotic Initiation Factor 2alpha Kinase and the Role of the Regulatory Motif in Heme Sensing by Spectroscopic and Catalytic Studies of Mutant Proteins. *J. Biol. Chem.* **2008**, *283*, 18782–18791. [[CrossRef](#)]
11. Hirai, K.; Martinkova, M.; Igarashi, J.; Saiful, I.; Yamauchi, S.; El-Mashtoly, S.; Kitagawa, T.; Shimizu, T. Identification of Cys385 in the Isolated Kinase Insertion Domain of Heme-Regulated EIF2 Alpha Kinase (HRI) as the Heme Axial Ligand by Site-Directed Mutagenesis and Spectral Characterization. *J. Inorg. Biochem.* **2007**, *101*, 1172–1179. [[CrossRef](#)] [[PubMed](#)]
12. Miksanova, M.; Igarashi, J.; Minami, M.; Sagami, I.; Yamauchi, S.; Kurokawa, H.; Shimizu, T. Characterization of Heme-Regulated EIF2alpha Kinase: Roles of the N-Terminal Domain in the Oligomeric State, Heme Binding, Catalysis, and Inhibition. *Biochemistry* **2006**, *45*, 9894–9905. [[CrossRef](#)] [[PubMed](#)]
13. Igarashi, J.; Sato, A.; Kitagawa, T.; Yoshimura, T.; Yamauchi, S.; Sagami, I.; Shimizu, T. Activation of Heme-Regulated Eukaryotic Initiation Factor 2alpha Kinase by Nitric Oxide Is Induced by the Formation of a Five-Coordinate NO-Heme Complex: Optical Absorption, Electron Spin Resonance, and Resonance Raman Spectral Studies. *J. Biol. Chem.* **2004**, *279*, 15752–15762. [[CrossRef](#)]
14. Martinkova, M.; Igarashi, J.; Shimizu, T. Eukaryotic Initiation Factor 2alpha Kinase Is a Nitric Oxide-Responsive Mercury Sensor Enzyme: Potent Inhibition of Catalysis by the Mercury Cation and Reversal by Nitric Oxide. *FEBS Lett.* **2007**, *581*, 4109–4114. [[CrossRef](#)] [[PubMed](#)]
15. Yerlikaya, A. Heme-Regulated Inhibitor: An Overlooked EIF2 α Kinase in Cancer Investigations. *Med. Oncol.* **2022**, *39*, 73. [[CrossRef](#)] [[PubMed](#)]
16. Girardin, S.E.; Cuziol, C.; Philpott, D.J.; Arnoult, D. The EIF2 α Kinase HRI in Innate Immunity, Proteostasis, and Mitochondrial Stress. *FEBS J.* **2021**, *288*, 3094–3107. [[CrossRef](#)] [[PubMed](#)]
17. Abdel-Nour, M.; Carneiro, L.A.M.; Downey, J.; Tsalikis, J.; Outlioua, A.; Prescott, D.; Da Costa, L.S.; Hovingh, E.S.; Farahvash, A.; Gaudet, R.G.; et al. The Heme-Regulated Inhibitor Is a Cytosolic Sensor of Protein Misfolding That Controls Innate Immune Signaling. *Science* **2019**, *365*, eaaw4144. [[CrossRef](#)] [[PubMed](#)]

18. Mukai, K.; Shimizu, T.; Igarashi, J. Phosphorylation of a Heme-Regulated Eukaryotic Initiation Factor 2 α Kinase Enhances the Interaction with Heat-Shock Protein 90 and Substantially Upregulates Kinase Activity. *Protein Pept. Lett.* **2011**, *18*, 1251–1257. [[CrossRef](#)]
19. Igarashi, J.; Sasaki, T.; Kobayashi, N.; Yoshioka, S.; Matsushita, M.; Shimizu, T. Autophosphorylation of Heme-Regulated Eukaryotic Initiation Factor 2 α Kinase and the Role of the Modification in Catalysis. *FEBS J.* **2011**, *278*, 918–928. [[CrossRef](#)]
20. Shugar, D. The NTP Phosphate Donor in Kinase Reactions: Is ATP a Monopolist? *Acta Biochim. Pol.* **1996**, *43*, 9–23. [[CrossRef](#)]
21. Greenman, C.; Stephens, P.; Smith, R.; Dalgliesh, G.L.; Hunter, C.; Bignell, G.; Davies, H.; Teague, J.; Butler, A.; Stevens, C.; et al. Patterns of Somatic Mutation in Human Cancer Genomes. *Nature* **2007**, *446*, 153–158. [[CrossRef](#)] [[PubMed](#)]
22. Palrecha, S.; Lakade, D.; Kulkarni, A.; Pal, J.K.; Joshi, M. Computational Insights into the Interaction of Small Molecule Inhibitors with HRI Kinase Domain. *J. Biomol. Struct. Dyn.* **2019**, *37*, 1715–1723. [[CrossRef](#)]
23. White, J.C.; Capizzi, R.L. A Critical Role for Uridine Nucleotides in the Regulation of Deoxycytidine Kinase and the Concentration Dependence of 1-Beta-D-Arabinofuranosylcytosine Phosphorylation in Human Leukemia Cells. *Cancer Res.* **1991**, *51*, 2559–2565. [[PubMed](#)]
24. Traut, T.W. Physiological Concentrations of Purines and Pyrimidines. *Mol. Cell Biochem.* **1994**, *140*, 1–22. [[CrossRef](#)] [[PubMed](#)]
25. Ricketts, M.D.; Emptage, R.P.; Blobel, G.A.; Marmorstein, R. The Heme-Regulated Inhibitor Kinase Requires Dimerization for Heme-Sensing Activity. *J. Biol. Chem.* **2022**, *298*, 102451. [[CrossRef](#)]
26. Pytel, D.; Seyb, K.; Liu, M.; Ray, S.S.; Concannon, J.; Huang, M.; Cuny, G.D.; Diehl, J.A.; Glicksman, M.A. Enzymatic Characterization of ER Stress-Dependent Kinase, PERK, and Development of a High-Throughput Assay for Identification of PERK Inhibitors. *J. Biomol. Screen.* **2014**, *19*, 1024–1034. [[CrossRef](#)]
27. McKenna, S.A.; Lindhout, D.A.; Kim, I.; Liu, C.W.; Gelev, V.M.; Wagner, G.; Puglisi, J.D. Molecular Framework for the Activation of RNA-Dependent Protein Kinase. *J. Biol. Chem.* **2007**, *282*, 11474–11486. [[CrossRef](#)] [[PubMed](#)]
28. Mellor, H.; Proud, C.G. A Synthetic Peptide Substrate for Initiation Factor-2 Kinases. *Biochem. Biophys. Res. Commun.* **1991**, *178*, 430–437. [[CrossRef](#)]
29. Yamada, S.; Nakamura, H.; Kinoshita, E.; Kinoshita-Kikuta, E.; Koike, T.; Shiro, Y. Separation of a Phosphorylated Histidine Protein Using Phosphate Affinity Polyacrylamide Gel Electrophoresis. *Anal. Biochem.* **2007**, *360*, 160–162. [[CrossRef](#)]

Disclaimer/Publisher’s Note: The statements, opinions and data contained in all publications are solely those of the individual author(s) and contributor(s) and not of MDPI and/or the editor(s). MDPI and/or the editor(s) disclaim responsibility for any injury to people or property resulting from any ideas, methods, instructions or products referred to in the content.